Advances in Nano Research, *Vol. 14, No. 6 (2023) 575-590*
https://doi.org/10.12989/anr.2023.14.6.575

Computational thermal stability and critical temperature buckling of nanosystem

Chengda Zhang, Haifeng Hu, Qiang Ma and Ning Wang*

School of Navigation, Shandong Jiaotong University, Jinan 264003, Shandong, China

(*Received March 16, 2022, Revised August 17, 2022, Accepted August 23, 2022*)

Abstract. Many of small-scale devices should be designed to tolerate high temperature changes. In the present study, the states of buckling and stability of nano-scale cylindrical shell structure integrated with piezoelectric layer under various thermal and electrical external loadings are scrutinized. In this regard, a multi-layer composite shell reinforced with graphene nano-platelets (GNP) having different patterns of layer configurations is modeled. An outer layer of piezoelectric material receiving external voltage is also attached to the cylindrical shell for the aim of observing the effects of voltage on the thermal buckling condition. The cylindrical shell is mathematically modeled with first-order shear deformation theory (FSDT). Linear elasticity relationship with constant thermal expansion coefficient is used to extract the relationship between stress and strain components. Moreover, minimum virtual work, including the work of the piezoelectric layer, is engaged to derive equations of motion. The derived equations are solved using numerical method to find out the effects of temperature and external voltage on the buckling stability of the shell structure. It is revealed that the boundary condition, external voltage and geometrical parameter of the shell structure have notable effects on the temperature rise required for initiating instability in the cylindrical shell structure.
Keywords: critical temperature; critical voltage; graphene nanoplatelets; maxwell's equation; piezoelectric layer

1. Introduction

Applications of small-systems are growing with an astonishing speed in different aspects of technology and also in our daily life. Health-care sensors, motion sensors, motion controls (Du *et al*. 2023, Fu *et al*. 2023, Shi *et al*. 2023), fluid transferring system are among the many of applications of these systems which are proven to be highly reliable (Guan *et al*. 2020, Ning *et al*. 2021, Sheng *et al*. 2021). The application of small-systems in different thermal, chemical, electrical environments needs delicate mathematical and experimental investigations (Xiong *et al*. 2020, Zhou *et al*. 2022, Zhu and Zhao 2022). In this regard, there are many research studies in examining and prediction of nan-structure behavior in such environments (Tong *et al*. 2016, Zhang *et al*. 2016, Gong *et al*. 2022).

Mechanical stability analysis of small-scale structures is of important since instable system could not perform their proposed tasks properly (Ji *et al*. 2017, Wang *et al*. 2018, Wu *et al*. 2021). Therefore, stability under various dynamic, static and thermal loadings have been investigated in structural element using mathematical approaches (Huang *et al*. 2022, Zhang *et al*. 2022b,c). Habibi *et al*. (2019d) presented vibrational stability analysis of cylindrical micro-shells under applied voltage to its piezoelectric patches. They utilized Hamilton's principle to derive equations of motion and boundary conditions of the structure (Dai *et al*. 2023a, b, Peng *et al*. 2023, Sabzevari *et al*. 2023, Shariati *et al*. 2023, Xiang *et al*. 2023, Yang *et al*. 2023, Zhang *et al*. 2023, Zhao *et al*. 2023, Zheng *et al*. 2023). The derived differential equations were solved numerically using generalized differential quadrature method (GDQM). The results of the study indicated that state of boundary condition and lamina patterns had significant effect on the critical external voltage causing vibrational instability in the cylindrical shell structure. Safarpour *et al*. (2018a) considered thermal effects in wave propagation in nano-scale composite cylindrical shells. To capture the small-scale effects in the structure, nonlocal strain gradient had been engaged in the dynamic analysis of the structure (Zhang *et al*. 2016, 2022a, Sun *et al*. 2023). The composite structure was made from GNP-reinforces layers with different patterns. Effects of temperature differences and wave number on the phase velocity of the structure were scrutinized in detail. Moreover, distribution pattern of GPL-reinforced layers' effects on the vibrational behavior of the nanoscale cylindrical shell (Wei *et al*. 2022, Yang *et al*. 2022c, Ren *et al*. 2023). Owing to small-scale effects, modified length-couple stress theory along with Hamilton's principle was utilized to model the motion of the structure. Numerical solutions for differential equations developed via size-dependent theories are widespread in the field of structural mechanics. Mohammadi *et al*. (2019) utilized GDQM to solve differential equations of micro-scale cylindrical shell equations to delve into the dynamic responses of double wall cylindrical shell. The equations of motion in this case were established employing modified strain gradient theory and the displacement field components were obtained via first-order shear deformation theory. In their study, they consider functionally grading properties in the thickness of the cylinder. The outcome of the study indicated that natural frequency has been affected

*Corresponding author, Ph.D.,
E-mail: sdjtuedu@163.com

ISSN: 2287-237X (Print), 2287-2388 (Online)

by geometrical and material parameters.

Nonlinear and large deformation behavior in structures occur in actual problem (Lu *et al*. 2021, Zhou *et al*. 2021, Zhao *et al*. 2022) and it is more beneficial and accurate taking into consideration the nonlinear terms of displacement and strain components into account. Hou *et al*. (Hou *et al*. 2021b) examined static response and stability behavior of mechanical structures made from GPL-reinforced composite under static loadings. The composite material were graded in one direction. Large deflection equations were obtained by assuming von-Karman theory and modified couple stress theory. The nonlinear differential equations were solve using semi-analytical method of homotopy perturbation. Xu *et al*. (2021b) explored the nonlinear vibration of cylindrical shell with non-uniform cross section under harmonic forces. The modified couple stress theory and von-Karman large deflection theory for shell structures were engaged to obtain the relation between stress components and displacement. The nonlinear equation were further solved by homotopy perturbation method. The effects of boundary condition and nonlinearity in the shell structure were shown to be considerable. There exist other novel methodologies in solving differential equations of vibration in structural mechanics. For an account, Jiao *et al*. (2021) utilized particle swarm optimization and genetic algorithm to solve magneto-electro-elastic equations of plates in nano-scale. State space modeling of nano-scale structure was performed by Zhao *et al*. (2021) in the problem modeling of rotating annular disk structure. Dong *et al*. (2022) utilized novel method of combining general differential quadrature and finite element methods to solve the equations of motion for conical shell structure. Controlling of vibration in small-scale structure was the focus of many research articles. Moradi *et al*. (2021) tried to design a system to control vibration of nano-composite cylindrical structure using piezoelectric sensor and actuator. It was demonstrated that using PD controller in such system could widen the stability region and improve the vibration properties of the system. Chaotic motion of annular plate in nano-scale structure is the subject of an article by Ma *et al*. (2021). Nonlinear deformation equation of the plate were derived using von-Karman relations and GDQM method was the numerical solution strategy in their paper. It was shown that the weight fraction of the reinforcement in the composite material is highly important in determining chaotic response of the structure. Moreover, some geometrical aspect ratios of the structure has been proven to have insignificant effect on the nonlinear frequency of the annular structure. Dynamic instability of rotating beam structure is considered in a work by Yang *et al*. (2022b). In the solution procedure of the driven equations of motion Chebyshev–Ritz path had been utilized. The nonlinear equations were further solved using Newton-Raphson method.

Wave propagation is one of the other aspects of the nano-scale structures (Habibi *et al*. 2016, 2017, 2018a, b, 2019a, b, c, d, Safarpour *et al*. 2018b, 2019a, b, 2020, Ebrahimi *et al*. 2019a, c, 2020a, Esmailpoor Hajilak *et al*. 2019, Pourjabari *et al*. 2019, Alipour *et al*. 2020, Ghazanfari *et al*. 2020, Chen *et al*. 2022, Zhu *et al*. 2022). Al-Furjan *et al*. (2020g) exploited four different continuum elasticity theory to observe the wave propagation patterns in cylindrical nano-shells made from composite lamina. Effects of angular velocity and lamina pattern had important influence on the wave propagation in the cylindrical shell. Scale influence on the wave dispersion in carbon nano tube structures was explored by Wang *et al*. (2006) using nonlocal elasticity theory. The effect of the tubes diameter on the vibration of carbon nanotube was shown using analytical solution. In addition, different modeling approaches were discussed and compared.

In this sense, the current study is devoted to analyzing state of buckling and stability of nano-scale cylindrical shell structure integrated with piezoelectric layer under various thermal and electrical external loading. In this regard, a multi-layer composite shell reinforced with graphene nano-platelets (GNP) having different patterns of layer configurations is considered. An outer layer of piezoelectric material receiving external voltage is also attached to the cylindrical shell for the aim of observing effects of voltage of the thermal buckling condition. The cylindrical shell is mathematically modeled with first-order shear deformation theory (FSDT). Linear elasticity relationship with constant thermal expansion coefficient is used to extract the relationship between stress and strain components. Moreover, minimum virtual work, including the work of the piezoelectric layer, is engaged to derive equations of motion. The derived equations are solved using numerical method to find out the effects of temperature and external voltage on the buckling stability of the shell structure.

2. Mathematical formulation of multilayer GNP reinforced composite

The geometry of cylindrical multilayer composite shell is illustrated in Fig. 1. The composite layers could be designed to have different configuration. In addition, a piezoelectric layer is attached to the outer layer of the cylinder for the purpose of applying electrical voltage. The length of the cylinder is denoted by L and its radius by R. The thickness of the composite is sum of thicknesses of multilayer GNP-RC and thickness of the piezoelectric layer, $h_{eff} = h + h_p$. The piezoelectric layer exposed to an electrical voltage of V. In addition, the whole structure is exposed to a thermal environment which applies temperature change to the structure. It is expected, thermal and electrical loadings along with different boundary condition change the critical condition of buckling in cylindrical shell. In addition to the layers patterns shown in this figure, a uniform pattern is also considered having same weight fraction of GNP in all layers.

2.1 GNPRC composite core

For different layer patterns in composite lamina, the effective volume fraction of GNP is calculated differently. In each layer k the GNP volume fraction $V_G(k)$ is designed to be a function of the total volume fraction V_G^* as *al*. 2019, Moayedi *et al*. 2019, 2020a, b, Mohammadgholiha

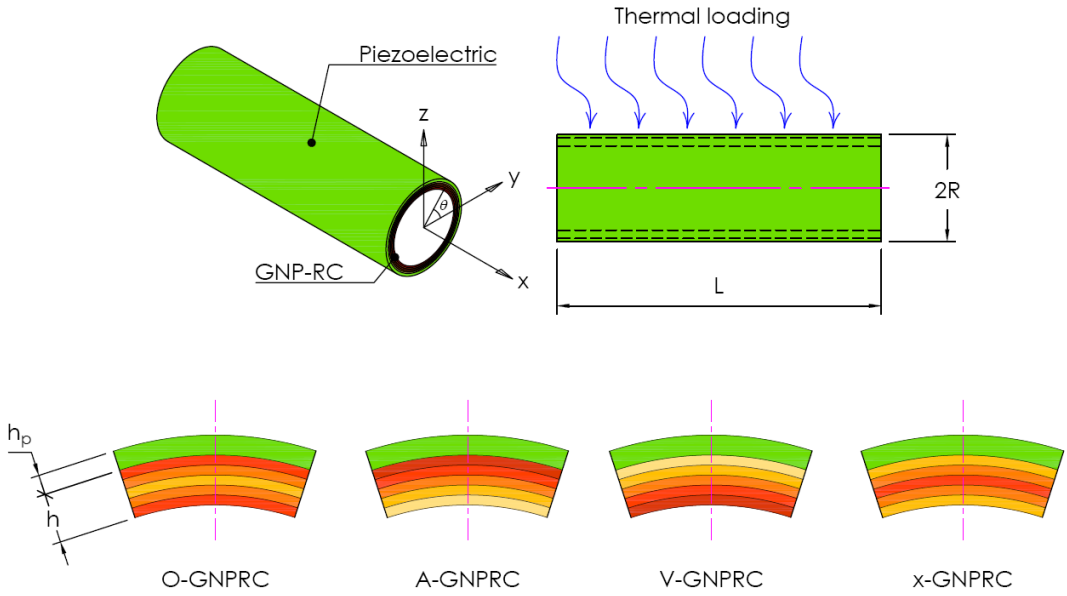

Fig. 1 Multilayer composite cylindrical shell structure with different layers patterns

et al. 2019, Mohammadi *et al*. 2019, Habibi *et al*. 2020, Oyarhossein *et al*. 2020, Shariati *et al*. 2020a, b, Shokrgozar *et al*. 2020):

$$U-GNPRC: V_G(k) = V_G^* \tag{1}$$

$$X-GNPRC: V_G(k) = 2V_G^* \frac{|2k - N_L - 1|}{N_L} \tag{2}$$

$$O-GNPRC: V_G(k) = 2V_G^* \left(1 - \frac{|2k - N_L - 1|}{N_L}\right) \tag{3}$$

$$A-GNPRC: V_G(k) = 2V_G^* \frac{2k - 1}{N_L} \tag{4}$$

In the above formula, N_L is the total number of layers. In addition, the total volume fraction can be calculated from the mass density and weight fraction of GNP g_{GPN} (Hashemi *et al*. 2019, Al-Furjan *et al*. 2020c, d, e, f, Bai *et al*. 2020, Cheshmeh *et al*. 2020, Li *et al*. 2020a, Lori *et al*. 2020, Najaafi *et al*. 2020, Shariati *et al*. 2020c, Xiong *et al*. 2020, Guo *et al*. 2021b, Liu *et al*. 2021a):

$$V_G^* = \frac{g_{GNP}}{g_{GNP}\left(1 - \frac{\rho_{GNP}}{\rho_m}\right) + \frac{\rho_{GNP}}{\rho_m}} \tag{5}$$

where ρ_m and ρ_{GNP} are the densities of mass for matrix and GNP, respectively. For randomly distributed GNP filler in the polymer matric, Halpin-Tsai model suggested the following approximate relations (Song *et al*. 2017):

$$\begin{aligned} E &= \frac{5}{8}E_T + \frac{3}{8}E_L, \\ E_T &= \frac{1 + \xi_T n_T V_G}{1 - n_T V_G} E_m, E_L = \frac{1 + \xi_L n_L V_G}{1 - n_L V_G} E_m \end{aligned} \tag{6}$$

where E, E_T *and* E_L are the effective, transversal and longitudinal moduli of elasticity in composite layer made given below (Ebrahimi *et al*. 2019b, c, 2020b, Hashemi *et* from polymer matric and GNP reinforcements. There are other parameters in Eq. (6) which are defined as (Adamian *et al*. 2020, Al-Furjan *et al*. 2020a, b, Li *et al*. 2020b, Liu *et al*. 2020b, 2021b, Zare *et al*. 2020, Dai *et al*. 2021b, Habibi *et al*. 2021, He *et al*. 2021, Huang *et al*. 2021a, Zhang *et al*. 2021):

$$\begin{aligned} &\xi_L = 2(l_G/h_G), \xi_t = 2(b_G/h_G), \\ &n_L = \frac{(E_G/E_m) - 1}{(E_G/E_m) + \xi_L}, n_T = \frac{(E_G/E_m) - 1}{(E_G/E_m) + \xi_T} \end{aligned} \tag{7}$$

Two parameters ξ_T and ξ_L are the GNPs geometrical parameters and where l_G, b_G, h_G are the average length, width and thickness of the GNPs. Modulus of elasticity of GNPs is denoted by E_G. Using rule of mixture, the following relations could be utilized in calculation of equivalent elastic constants, thermal expansion coefficient and mass density of the composite lamina (Liu *et al*. 2020a, Wang *et al*. 2020, Zhou *et al*. 2020, Dai *et al*. 2021a, Guo *et al*. 2021a, Shao *et al*. 2021, Wu and Habibi 2021, Kong *et al*. 2022):

$$\begin{aligned} E &= E_G V_G + E_M V_M, \\ \rho &= \rho_G V_G + \rho_M V_M, \\ \nu &= \nu_G V_G + \nu_M V_M, \\ \alpha &= \alpha_G V_G + \alpha_M V_M. \end{aligned} \tag{8}$$

In the above equations $V_M = 1 - V_G$ (Ma *et al*. 2022, Zhao *et al*. 2022, Hou *et al*. 2021a, Huang *et al*. 2021b, c, Jiao *et al*. 2021, Liu *et al*. 2021c, Moradi *et al*. 2021, Xu *et al*. 2021a, Dong *et al*. 2022, Luo *et al*. 2022a, Michael *et al*. 2022, Wang *et al*. 2022c, Yang *et al*. 2022b, Yu *et al*. 2022).

2.2 Mathematical modeling of the core

Using first-order shear deformation theory, the following relations could be given for the displacement components in the multilayer composite core (Gu *et al*. , Xu

et al. 2022, Yang *et al*. 2022d). It is noteworthy that the bonding between layers is assumed to be perfect in both normal and tangential directions:

$$\begin{aligned} u^c(\theta,x,z,t) &= u_0^c(\theta,x,t) + z\chi_x^c(\theta,x,t) \\ v^c(\theta,x,z,t) &= v_0^c(\theta,x,t) + z\chi_\theta^c(\theta,x,t) \\ w^c(\theta,x,z,t) &= w_0^c(\theta,x,t) \end{aligned} \tag{9}$$

where, u_0^c, v_0^c and w_0^c represent the displacements in axial circumferential and radial-directions on the central surface of the composite core, respectively. Two functions $\chi_x^c$and χ_θ^c are the rotation angles of the initial normal to the middle plane with the current normal about the axial and circumferential directions (Fan *et al*. 2022, Luo *et al*. 2022b, Michael *et al*. 2022, Wang *et al*. 2022b, c, Yang *et al*. 2022a, Zheng *et al*. 2022, Zhu *et al*. 2022).

2.3 Constitutive equations for composite core

The linear elastic behavior is considered to model the relationship between stress and strain components. Considering uniform temperature change throughout the inner multilayer composite, following relation could be readily written:

$$\begin{bmatrix} s_{xx}^c \\ s_{\theta\theta}^c \\ s_{x\theta}^c \\ s_{xz}^c \\ s_{\theta z}^c \end{bmatrix} = \begin{bmatrix} \tilde{E}_{11} & \tilde{E}_{12} & 0 & 0 & 0 \\ \tilde{E}_{21} & \tilde{E}_{22} & 0 & 0 & 0 \\ 0 & 0 & \tilde{E}_{66} & 0 & 0 \\ 0 & 0 & 0 & \tilde{E}_{55} & 0 \\ 0 & 0 & 0 & 0 & \tilde{E}_{44} \end{bmatrix} \times \begin{bmatrix} e_{xx}^c - \alpha_1 \Delta T \\ e_{\theta\theta}^c - \alpha_2 \Delta T \\ e_{x\theta}^c \\ e_{xz}^c \\ e_{\theta z}^c \end{bmatrix} \tag{10}$$

It should be noticed that in the shell structure, the total thickness is much smaller than the radius and length of the cylinder so that the stress in the normal direction could be considered constant. The constants α_i are the thermal expansion in the first and second principal direction of the cylinder. Moreover, variable ΔT is the uniform temperature change in the composite layers. The values of constants $\tilde{E}_{ij}$ are presented in detail in Ref. (Ghadiri and Safarpour 2016) and further explanation of these constants are omitted here.

2.4 Mathematical modeling of the piezoelectric layer

Similar to the multilayer composite of the inner layer in the cylindrical shell, for the piezoelectric layer the following displacement field is given based on the FSDT:

$$\begin{aligned} u^p(\theta,x,z,t) &= u_0^p(\theta,x,t) + z\chi_x^p(\theta,x,t) \\ v^p(\theta,x,z,t) &= v_0^p(\theta,x,t) + z\chi_\theta^p(\theta,x,t) \\ w^p(\theta,x,z,t) &= w_0^p(\theta,x,t) \end{aligned} \tag{11}$$

in which u_0^p, v_0^p and w_0^p denote the displacements of the middle surface in x, θ and z directions of the piezoelectric layer, respectively Two functions χ_x^p and χ_θ^p are the rotation angles of the initial normal to the middle plane of the piezoelectric layer with the current normal about the axial and circumferential directions. Having the displacement field, we could now calculate the strain tensor components assuming small deformation and rotation in the structure using the following relation in the cylindrical coordinate system:

$$\begin{aligned} e_{xx}^p &= z\frac{\partial \chi_x^p}{\partial x} + \frac{\partial u_0^p}{\partial x} \\ e_{\theta\theta}^p &= \frac{1}{R_p}\frac{\partial v_0^p}{\partial \theta} + \frac{w_0^p}{R_p} + \frac{z}{R_p}\frac{\partial \chi_\theta^p}{\partial \theta} \\ e_{xz}^p &= \frac{1}{2}\left(\frac{\partial w_0^p}{\partial x} + \chi_x^p\right) \\ e_{x\theta}^p &= \frac{1}{2}\left(\frac{\partial v_0^p}{\partial x} + \frac{1}{R_p}\frac{\partial u_0^p}{\partial \theta}\right) + \frac{z}{2}\left(\frac{\partial \chi_\theta^p}{\partial x} + \frac{1}{R_p}\frac{\partial \chi_x^p}{\partial \theta}\right) \\ e_{\theta z}^p &= \frac{1}{2}\left(\chi_\theta^p - \frac{v^p}{R_p} + \frac{1}{R_p}\frac{\partial w^p}{\partial \theta}\right) \end{aligned} \tag{12}$$

2.5 Constitutive equations for piezoelectric layer

The stress tensor components in the piezoelectric layer are not only dependent on the state of deformation owing to mechanical forces but also are relied on the deformation induced by external applied electrical voltage. In this layer, the effect of temperature change is neglected:

$$\begin{Bmatrix} s_{xx}^p \\ s_{\theta\theta}^p \\ s_{x\theta}^p \\ s_{\theta z}^p \\ s_{xz}^p \end{Bmatrix} = \begin{bmatrix} c_{11} & c_{12} & 0 & 0 & 0 \\ c_{12} & c_{22} & 0 & 0 & 0 \\ 0 & 0 & c_{66} & 0 & 0 \\ 0 & 0 & 0 & c_{55} & 0 \\ 0 & 0 & 0 & 0 & c_{44} \end{bmatrix} \cdot \begin{bmatrix} e_{xx}^p \\ e_{\theta\theta}^p \\ e_{x\theta}^p \\ e_{\theta z}^p \\ e_{xz}^p \end{bmatrix} - \begin{bmatrix} 0 & 0 & q_{31} \\ 0 & 0 & q_{32} \\ 0 & 0 & 0 \\ 0 & q_{24} & 0 \\ q_{25} & 0 & 0 \end{bmatrix} \begin{Bmatrix} E_x \\ E_\theta \\ E_z \end{Bmatrix} \tag{13}$$

$$\begin{Bmatrix} D_x \\ D_\theta \\ D_z \end{Bmatrix} = \begin{bmatrix} 0 & 0 & 0 & 0 & q_{15} \\ 0 & 0 & 0 & q_{24} & 0 \\ q_{31} & q_{32} & 0 & 0 & 0 \end{bmatrix} \cdot \begin{Bmatrix} s_{xx}^p \\ s_{\theta\theta}^p \\ s_{x\theta}^p \\ s_{\theta z}^p \\ s_{xz}^p \end{Bmatrix} + \begin{bmatrix} r_{11} & 0 & 0 \\ 0 & r_{22} & 0 \\ 0 & 0 & r_{33} \end{bmatrix} \begin{Bmatrix} E_x \\ E_\theta \\ E_z \end{Bmatrix} \tag{14}$$

In these equations, constants c_{ij} are elasticity constants of the piezoelectric material and q_{ij} are the component

piezoelectric tensor and r_{ij} are the components of permittivity of the material. In addition two vector D_i and E_i are the electric flux density and the electric field strength, respectively. The electric field strength components is calculated using a potential function $\widetilde{\mathbf{\Upsilon}}$, as follows:

$$\begin{aligned} E_x &= -\widetilde{\Upsilon}_{,x} \\ E_\theta &= \frac{-\widetilde{\Upsilon}_{,\theta}}{R+z} \\ E_z &= -\widetilde{\Upsilon}_{,z}. \end{aligned} \tag{15}$$

In the present article, the following form foe the electric potential field is adopted from Wang (2002):

$$\widetilde{\Upsilon}(\theta,x,z,t) = -cos(\beta z)\Upsilon(\theta,x,t) + \frac{2z\Upsilon_0}{h} \tag{16}$$

In which $\beta=\pi/h$, Υ_0 is the initial external electric potential.

2.6 Compatibility equations between core and piezoelectric layer

As mentioned above, the displacement in the interface of composite layers and between piezoelectric layer and composite layer is assumed to be perfect which concludes the following compatibility relations:

$$\begin{aligned} &u^c(z^c=h/2) = u^p(z^p=-h_p/2), \\ &v^c(z^c=h/2) = v^p(z^p=-h_p/2), \\ &w^c(z^c=h/2) = w^p(z^p=-h_p/2) \end{aligned} \tag{17}$$

If the above relation used in the FSDT displacement components, the following relation between displacement component in the interface of the piezoelectric layer and composite layers are derived (Khalili and Mohammadi 2012, Nasihatgozar and Khalili 2017, Pourmoayed *et al.* 2017):

$$\begin{aligned} u_0^p &= \frac{h}{2}\chi_x^p + u_0^c + \frac{h}{2}\chi_x^c \\ v_0^p &= \frac{h}{2}\chi_\theta^p + v_0^c + \frac{h}{2}\chi_\theta^c \\ w_0^p &= w_0^c \end{aligned} \tag{18}$$

2.7 Motion and boundary equations for GNPRC cylindrical shell coupled with PIAC

The principle of minimum virtual work (Shariati *et al*. 2012, 2016a, b, 2019, 2020d, e, f, g, h, i, j, 2021a, b, Fan *et al*. 2022, Luo *et al*. 2022b, Wang *et al*. 2022a, Xia *et al*. 2022) also known as Hamilton's principle is engaged in this section to obtain the equations of motion based on stress and displacement components. The fundamental relation of this principle is:

$$\int_{t_1}^{t_2} \delta U - \delta W_1 - \delta W_2 = 0 \tag{19}$$

Each component of the above equation could be calculated using their definitions as follows:

$$\begin{aligned} U = &\frac{1}{2}\int_{V_c} (s_{pq}\delta e_{pq}) dV_{core} \\ &- \int_{V_p} (D_\theta \delta E_\theta + D_x \delta E_x + D_z \delta E_z) dV_p \end{aligned} \tag{20}$$

Here, tensors e_{ij} and s_{ij} indicate the components of strain and stress tensors, respectively as calculated in the previous sections The first external work from applied electrical voltage could be written as:

$$\delta W_1 = \iint_A \left[(H_1^P) w_{,x} \delta w_{,x} + (H_2^P) v_{,x} \delta v_{,x}\right] R_p d\theta dx \tag{21}$$

where N_i^P is external electric loads. The electric loads could be obtained as follows (Ke *et al*. 2014):

$$H_1^P = H_2^P = -2(q_{31} - \frac{c_{13}q_{33}}{c_{33}})\Upsilon_0 \tag{22}$$

In addition, the second part of external work comes from change in the environment temperature which inducing the following work term in the cylindrical structure:

$$W_2 = \frac{1}{2}\iint_A \left[(H_1^T)(\frac{\partial w_0^c}{\partial x})^2 + (H_2^T)(\frac{\partial v_0^c}{\partial x})^2\right] R_c d\theta dx \tag{23}$$

where N_1^T and N_2^T are the thermal resultants which can be obtained as follows:

$$\begin{aligned} H_1^T &= \int_{-h_c/2}^{h_c/2} (\tilde{E}_{11} + \tilde{E}_{12})\alpha(T-T_0) dz_c, \\ H_2^T &= \int_{-h_c/2}^{h_c/2} (\tilde{E}_{21} + \tilde{E}_{22})\alpha(T-T_0) dz_c. \end{aligned} \tag{24}$$

Thermal expansion coefficients are combined in a vector form as given below:

$$\alpha = [\alpha_1 \alpha_2 000]^T \tag{25}$$

It is assumed that the temperature varies linearly along the thickness from T_m at the outer surface to T_c at the inner surface. Substituting Eqs. (20), (21) and (23) into Eq. (19) and integrating part by part, the motion equations can be extract as follows:

$$\delta u_c: H_{xx,x}^c + \frac{H_{x\theta,\theta}^c}{R_c} = 0, \tag{26}$$

$$\delta v_c: H_{x\theta,x}^c + \frac{H_{\theta\theta,\theta}^c}{R_c} + \frac{Q_{z\theta}^c}{R_c} - (H_1^T) v_{0,xx} = 0 \tag{27}$$

$$\delta w_c: Q_{xz,x}^c + \frac{Q_{z\theta,\theta}^c}{R_c} - \frac{H_{\theta\theta}^c}{R_c} - (H_1^T) w_{0c,xx} = 0, \tag{28}$$

$$\delta \chi_x^c: F_{xx,x}^c + \frac{F_{\theta\theta,\theta}^c}{R_c} - Q^c{}_{xz} = 0, \tag{29}$$

$$\delta \chi_\theta^c: \frac{F_{\theta\theta,\theta}^c}{R_c} + F_{x\theta,x}^c - Q_{z\theta}^c = 0. \tag{30}$$

$$\delta u_0^p: \frac{\partial H_{xx}^p}{\partial x} + \frac{1}{R_p}\frac{\partial H_{x\theta}^p}{\partial \theta} + T_{31}\chi_{,x} = 0 \tag{31}$$

$$\delta v_0^p: \frac{\partial H_{x\theta}^p}{\partial x} + \frac{1}{R_p}\frac{\partial H_{\theta\theta}^p}{\partial \theta} + \frac{Q_{z\theta}^p}{R_p} + \frac{T_{61}^p}{R_p}\chi_{,\theta} - \frac{k_s T_{24}^p}{R_p}\phi_{,\theta} - (H_1^p)v_{0p,xx} = 0 \tag{32}$$

$$\delta w_0^p: -k_s T_{15}\chi_{,xx} - (H_1^p)w_{0p,xx} + \frac{\partial H_{xz}^p}{\partial x} + \frac{1}{R_p}\frac{\partial H_{z\theta}^p}{\partial \theta} - \frac{H_{\theta\theta}^p}{R_p} - \frac{k_s X_{24}^p}{R_p}\chi_{,\theta\theta} = 0, \tag{33}$$

$$\delta u_1^p: -Q^p{}_{xz} + T_{32}\chi_{,x} + k_s T_{12}\chi_{,x} + \frac{\partial F_{xx}^p}{\partial x} + \frac{1}{R_p}\frac{\partial F_{\theta\theta}^p}{\partial \theta} = 0, \tag{34}$$

$$\delta v_1^p: -Q^p{}_{z\theta} + \frac{T_{62}}{R_p}\chi_{,\theta} + k_s T_{13}\chi_{,\theta} + \frac{1}{R_p}\frac{\partial F_{\theta\theta}^p}{\partial \theta} + \frac{\partial F_{x\theta}^p}{\partial x} = 0 \tag{35}$$

The motion equation related to the piezoelectric layer can be written as follows:

$$\delta\Upsilon: \int_{-h_p/2}^{h_p/2} \left\{ \begin{matrix} D_{x,x}\, cos(\frac{\pi}{h}z) + D_{\theta,\theta}\frac{cos(\frac{\pi}{h}z)}{R_p + z} \\ +D_z\beta\, sin(\frac{\pi}{h}z) \end{matrix} \right\} dz = 0 \tag{36}$$

In Eqs. (26)-(36), it is assumed that:

$$\begin{aligned} (H_{xx}^m, H_{\theta\theta}^m, H_{x\theta}^m) &= \int_{-h_i/2}^{h_i/2} (s_{xx}^m, s_{\theta\theta}^m, s_{x\theta}^m)dz, m = p, c \\ (F_{xx}^m, F_{\theta\theta}^m, F_{x\theta}^m) &= \int_{-h_i/2}^{h_i/2} (s_{xx}^m, s_{\theta\theta}^m, s_{x\theta}^m)zdz\,, m = p, c \\ (Q^m{}_{xz}, Q^m{}_{z\theta}) &= \int_{-h_i/2}^{h_i/2} k_s(s_{xz}^m, s_{z\theta}^m)dz\,, m = p, c \end{aligned} \tag{37}$$

Also, the parameters that used in Eq. (37) are expressed as:

$$\begin{aligned} &\int_{-h_p/2}^{h_p/2} D_x \cos(\frac{\pi}{h}z) \\ &= T_{11}\phi_{,x} + T_{12}(u_{1p} + w_{0\,p,x}), \\ &\int_{-h_p/2}^{h_p/2} D_\theta \frac{\cos(\frac{\pi}{h}z)}{R+z}dz \\ &= T_{22}\Upsilon_{,\theta} + T_{13}(v_1^p + \frac{1}{R_p}w_{0,\theta}^p - \frac{v_0^p}{R_p}), \\ &\int_{-h_p/2}^{h_p/2} D_z\beta \sin(\frac{\pi}{h}z)dz \\ &= -T_{33}\Upsilon + T_{31}u_{0,x}^p + T_{32}u_{1,x}^p \\ &+T_{61}(\frac{1}{R_p}v_{0,\theta}^p + \frac{w_0^p}{R_p}) + T_{62}(\frac{u_{1,\theta}^p}{R_p}). \end{aligned} \tag{38}$$

where:

$$\begin{aligned} T_{11} &= \int_{-h_p/2}^{h_p/2} \{q_{11e}\}(\cos(\beta z))^2 dz, X_{22} \\ &= \int_{-h_p/2}^{h_p/2} \{q_{22e}\}\left(\frac{\cos(\beta z)}{R_p + z}\right)^2 dz, \\ T_{13} &= \int_{-h_p/2}^{h_p/2} \frac{\cos(\frac{\pi}{h}z)}{R+z} e_{24e}dz,\ X_{33} \\ &= \int_{-h_p/2}^{h_p/2} \{q_{33e}\}\left(\frac{\pi}{h}\sin(\frac{\pi}{h}z)\right)^2 dz, \\ \{T_{31}, T_{32}\} &= \int_{-h_p/2}^{h_p/2} \{1, z_p\}\frac{\pi}{h}\sin(\frac{\pi}{h}z)\, r_{31e}dz, \\ \{T_{61}, T_{62}\} &= \int_{-h_p/2}^{h_p/2} \{1, z\}\frac{\pi}{h}\sin(\frac{\pi}{h}z)\, r_{32e}dz. \end{aligned} \tag{39}$$

The state of boundary condition should be carefully defined for different boundary conditions in terms of displacement and its derivatives. The clamped boundary conditions at $x = 0, L$:

$$\begin{aligned} &u_0^c = v_0^c = w_0^c = \chi_x^c = \chi_\theta^c = 0, \\ &\Upsilon = u_0^p = v_0^p = w_0^p = \chi_x^p = \chi_\theta^p = 0 \end{aligned} \tag{40}$$

The simply supported boundary conditions at $\theta = \pi/2$, $3\pi/2$:

$$\begin{aligned} &u_0^c = w_0^c = \chi_x^c = 0, v_0^c \neq 0, \chi_\theta^c \neq 0, \\ &\Upsilon = u_0^p = w_0^p = \chi_x^p = 0, v_0^p \neq 0, \chi_\theta^p \neq 0 \end{aligned} \tag{41}$$

3. Solution procedure:

In this section, a detailed description of the solution procedure is given. The differential equations obtained for the complicated structure and material models in the previous section need to be solved numerically. In this sense, the method of differential quadrature is selected for solving these equations and obtaining critical values for critical temperature causing buckling instability in the cylindrical structure. The essence of the differential quadrature method is grounded in assuming the derivatives of a function to be a linear combination of function's value in optimally specified points (Rajasekaran 2009):

$$\left.\frac{\partial^r g(x)}{\partial y^r}\right|_{x=x_p} = \sum_{j=1}^{n} \eta_{ij}^{(r)} g(y_i) \tag{42}$$

In the above equation, n is the number of specified points in which the function should be calculated. The coefficients η_{ij} are weight coefficient that should be calculated based on the optimization procedure. Using DQM have a merit over finite difference method of reducing calculation steps and increased accuracy. Following the Lagrange polynomial optimization procedure the weight coefficient could be calculated for the first derivative approximation as follows:

Table 1 Comparison of the effects of seed number on the critical temperature for different boundary condition and material combination. L/R=15, and h/R=0.1

B. Cs	Material	N=5	N=7	N=9	N=11	N=13	N=15
Simply-Simply	Pure epoxy	1258.659	1256.622	1256.856	1256.856	1256.856	1256.856
	Pattern 4	1785.632	1783.652	1783.652	1783.652	1783.652	1783.652
Clamped-Simply	Pure epoxy	1453.659	1452.365	1452.958	1452.958	1452.958	1452.958
	Pattern 4	2150.639	2148.326	2149.635	2149.635	2149.635	2149.635
Clamped-Clamped	Pure epoxy	1658.639	1654.236	1654.636	1654.636	1654.636	1654.636
	Pattern 4	2356.652	2355.659	2357.863	2357.863	2357.863	2357.863

$$\begin{aligned}&\eta_{ij}^{(1)}=\frac{\zeta(y_i)}{(y_i-y_j)\zeta(y_j)}\\&i,j=1,2,\dots,n \quad \text{and } i\neq j\\&\eta_{ij}^{(1)}=-\sum_{j=1,i\neq j}^{n}\eta_{ij}^{(1)}\ i=j\end{aligned} \tag{43}$$

where

$$\zeta(y_i)=\prod_{j=1,j\neq i}^{n}(y_i-y_j) \tag{44}$$

In the case of higher order derivatives r, the following recurrence relations are presented for weight coefficients:

$$\begin{aligned}&\eta_{ij}^{(r)}=r\eta_{ij}^{(r-1)}\left[\eta_{ij}^{(1)}-\frac{1}{(y_i-y_j)}\right]\\&i,j=1,2,\dots,n,i\neq j \quad \text{and } 2\leq r\leq n-1\\&\eta_{ii}^{(r)}=-\sum_{j=1,i\neq j}^{n}\eta_{ij}^{(r)}\\&i,j=1,2,\dots,n \quad \text{and } 1\leq r\leq n-1\end{aligned} \tag{45}$$

Selection of number of points or seeds is also dependent on the optimizing approach. The following seeds are selected to approximate of derivatives of functions:

$$y_i=\frac{L}{2}\left(1-cos\left(\frac{(i-1)}{(N_i-1)}\pi\right)\right)\ i=1,2,3,\dots,N_i \tag{46}$$

Since we are dealing with a symmetric structure, the following assumption for displacement function could be made:

$$\begin{aligned}&u_i(x,\theta,t)=U_i(x)\,cos(n\theta),i=c,p\\&v_i(x,\theta,t)=V_i(x)\,sin(n\theta),i=c,p\\&w_i(x,\theta,t)=W_i(x)\,cos(n\theta),i=c,p\\&\chi_x^i(x,\theta,t)=\Upsilon_x^i(x)\,cos(n\theta),i=c\\&\chi_\theta^i(x,\theta,t)=\Upsilon_\theta^i(x)\,sin(n\theta).i=c\end{aligned} \tag{47}$$

With some manipulation of the obtained equations in insertion of the boundary conditions, the following set of linear equation is obtained:

$$\left\{\begin{bmatrix}[f_{dd}] & [f_{db}]\\ [f_{bd}] & [f_{bb}]\end{bmatrix}N_{cr}+\begin{bmatrix}[k_{dd}] & [k_{db}]\\ [k_{bd}] & [k_{bb}]\end{bmatrix}\right\}\begin{Bmatrix}\delta_d\\ \delta_b\end{Bmatrix}=0 \tag{48}$$

In the above equation the subscript d indicated the domain grid point and b represents boundary grid point. At the end, dimensionless parameter is defined following Ref. (Ke *et al*. 2014):

$$\bar{\Upsilon}_{0cr}=\frac{10\times\Upsilon_{0cr}}{\sqrt{A_{11}/T_{33}}} \tag{49}$$

4. Results and discussion:

In this section, the results of numerical solutions are presented for a wide range of external applied voltage, boundary conditions and weight fraction of GNP to observe critical conditions leading to buckling of the structure.

4.1 Convergence

Since the DQM results are highly dependent on the seed numbers, a convergency study is performed for different boundary conditions to observe the rate of convergency for critical temperature and also to determine the minimum number of seeds required for further analyses in the following sections. The convergency results are provided in Table 1. As seen, for all cases of the different boundary condition at least 9 grid points is required in each direction to achieve reliable results. Therefore, in all the following analyses, at least 9 seeds will be used except otherwise stated.

4.2 Model validation:

The type of solution and problem geometry could be found in literature. Therefore, we select Ref. (Ghadiri and Safarpour 2016) for comparison of our result and, hence, validation of the procedure. The values for natural frequency of the structure given by the selected reference and as calculated using the approach in the current study are given in Table 2 for different applied voltages. As could be noted, the difference between calculated values are very small and therefore, the current approach could be confidently engaged for parametric analyzing.

4.3 Parametric results

It is discussed above that several parameter could affect the critical conditions for linear buckling occurrence. In this section, we aim to present the effect of each parameter and their importance in electro-thermal buckling (Wu *et al*. 2017).

Table 2 Comparison of the natural frequency calculated using the current method with the values obtained in Ref. (Ghadiri and Safarpour 2016)

Natural Frequency [THz]		Applied Voltage [mV]
Ref	Present	
0.02977	0.029878	-0.02
0.029619	0.029731	-0.015
0.029472	0.029577	-0.01
0.029323	0.029428	-0.005
0.029174	0.029279	0.000
0.029025	0.029127	0.005
0.028874	0.028975	0.01
0.02872	0.02882	0.015
0.028572	0.028664	0.02

Table 3 Comparison of critical temperature values in different values of $1/h_p$ and applied voltage for simply supported cylindrical shell structure

$1/h_p$	Applied voltage Φ			
	0.1mV	0.5mV	1mV	2mV
10	1374.17	1315.743	1205.282	1008.576
20	1024.472	948.9688	859.5573	662.852
30	899.2957	823.7927	728.4205	539.6629
40	839.6881	762.1981	666.0754	476.0814
50	799.9496	724.4466	632.816	440.3168
60	776.1066	701.5521	605.2313	412.4999
70	756.2374	686.031	585.3621	396.6045
80	744.3158	668.8128	573.4406	384.683
90	732.3943	656.8913	564.0798	372.7615

Table 4 Comparison of critical temperature values in different values of $1/h_p$ and applied voltage for clamped-simply cylindrical shell structure

$1/h_p$	Applied voltage Φ			
	0.1mV	0.5mV	1mV	2mV
10	2323.026	2248.726	2142.537	1954.084
20	1717.855	1643.536	1548.91	1354.221
30	1513.477	1433.849	1342.073	1149.843
40	1412.615	1334.141	1240.088	1048.981
50	1348.913	1271.939	1176.386	985.2789
60	1306.445	1232.125	1136.572	948.1193
70	1279.902	1202.928	1107.312	916.2682
80	1258.668	1179.04	1085.852	895.0341
90	1237.434	1161.636	1067.561	879.1085

4.4 Effects of applied voltage and piezoelectric thickness on critical temperature

Tables. 3, 4 and 5, variation of applied voltage and its effect on the critical voltage of cylindrical shell structure are provided for different values of piezoelectric layer thickness. It is observed that in all thicknesses of the piezoelectric layer, increase in the applied voltage causes decrease in the critical temperature required for destabilizing the structure. Hence, increase in the applied voltage deteriorate the stability condition of the cylindrical structure. On the other hand, increase in the thickness of the piezoelectric layer improve the stability through increasing critical temperature. These observations are hold for all boundary conditions.

However, there are some differences in the stability for different boundary conditions. From the value of the critical temperature in the same thickness and applied voltage, it could be concluded that the clamped-clamped boundary condition has superior stability over other two supposed BCs.

Table 5 Comparison of critical temperature values in different values of $1/h_p$ and applied voltage for fully clamed cylindrical shell structure

$1/h_p$	Applied voltage Φ			
	0.1mV	0.5mV	1mV	2mV
10	3615.75	3519.492	3431.221	3242.398
20	2674.129	2595.406	2500.949	2309.515
30	2363.378	2292.941	2197.343	1998.764
40	2206.831	2127.208	2036.054	1841.317
50	2113.607	2039.026	1936.614	1750.163
60	2048.484	1969.76	1874.464	1690.985
70	2002.907	1931.299	1836.812	1642.436
80	1969.76	1895.781	1803.605	1609.289
90	1940.757	1870.921	1770.88	1584.429

Table 6 Comparison of critical temperature in different values of g_{GPL} and applied voltage for simply supported cylindrical shell structure

g_{GNP}	Applied voltage Φ			
	0.1mV	0.5mV	1mV	2mV
0.1	603.7622	344.3696	24.06133	-300.748
0.5	637.3407	511.4114	354.1804	194.9591
1	652.7203	575.0999	483.6308	384.0343
1.5	662.6716	606.9442	539.2751	471.6061
2	672.4596	628.8371	575.0999	519.3725
2.5	678.5938	645.0691	598.9831	555.1972
3	686.5548	656.7008	616.8955	579.0804
3.5	692.5256	669.2391	633.1521	598.9831
4	698.4964	672.623	646.3666	614.7909

4.5 Effects of GNP weight fraction and applied voltage on critical temperature

Tables 6-8 in Tables 9- 11, variation of external applied voltage and its effect on the critical temperature of cylindrical shell structure are provided for different values of weight fraction of GNP. It is observed that in all weight fractions of GNP of the piezoelectric layer, increase in the

Table 7 Comparison of critical temperature in different values of g_{GPL} and applied voltage for clamped-simply cylindrical shell structure

g_{GNP}	Applied voltage Φ			
	0.1mV	0.5mV	1mV	2mV
0.1	1055.91	796.9981	470.5441	155.3471
0.5	1094.184	959.6292	808.6525	651.7161
1	1110.606	1035.118	941.7504	846.3966
1.5	1126.498	1071.67	1001.346	933.8042
2	1138.417	1096.435	1041.077	985.4541
2.5	1150.337	1114.579	1066.902	1027.171
3	1160.269	1130.471	1096.435	1051.01
3.5	1170.202	1148.218	1114.447	1076.835
4	1182.121	1158.283	1127.955	1098.687

Table 8 Comparison of critical temperature in different values of g_{GPL} and applied voltage for fully clamped cylindrical shell structure

g_{GNP}	Applied voltage Φ			
	0.1mV	0.5mV	1mV	2mV
0.1	1677.124	1417.771	1092.244	774.6608
0.5	1719.164	1592.144	1429.928	1276.982
1	1742.772	1668.507	1568.97	1473.958
1.5	1761.311	1705.695	1636.174	1571.287
2	1779.85	1735.82	1682.521	1626.904
2.5	1796.072	1763.629	1717.656	1673.252
3	1812.293	1779.85	1743.743	1705.695
3.5	1828.515	1803.024	1769.834	1738.138
4	1844.737	1821.563	1793.266	1763.629

Table 9 Comparison of critical voltage in different values of g_{GPL} and $1/h_p$ for simply-supported cylindrical shell structure

$1/h_p$	g_{GNP}			
	1%	0.5mV	1%	2mV
10	0.768493	0.799063	0.827902	0.855588
20	0.671016	0.70447	0.737347	0.767339
30	0.631795	0.668132	0.701586	0.736193
40	0.613338	0.650252	0.686451	0.718889
50	0.600648	0.638716	0.674477	0.708507
60	0.59315	0.631218	0.667556	0.702739
70	0.586806	0.626027	0.662431	0.696972
80	0.582768	0.621413	0.659046	0.693511
90	0.579307	0.617952	0.654866	0.69005

external applied voltage leads to reduction in the critical temperature required for destabilizing the structure. Hence, increase in applied voltage has a negative influence of the stability condition of the structure. On the other hand, increase in the weight fraction of GNP improve the stability through increasing critical temperature change. These

Table 10 Comparison of critical voltage in different values of g_{GPL} and $1/h_p$ for clamped-simply cylindrical shell structure

$1/h_p$	g_{GNP}			
	1%	1.2%	1.4%	1.6%
10	1.278682	1.329525	1.380354	1.42523
20	1.118177	1.175002	1.23083	1.283667
30	1.05537	1.118177	1.175002	1.231113
40	1.023469	1.088269	1.146091	1.204196
50	1.006452	1.070038	1.129143	1.187676
60	0.991567	1.058075	1.119023	1.175002
70	0.981598	1.049432	1.109204	1.168023
80	0.975616	1.041697	1.102226	1.162042
90	0.970588	1.035432	1.097241	1.157057

Table 11 Comparison of critical voltage in different values of g_{GPL} and $1/h_p$ for fully clamped cylindrical shell structure

$1/h_p$	g_{GNP}			
	1%	1.2%	1.4%	1.6%
10	1.978749	2.057258	2.13465	2.208326
20	1.729147	1.821319	1.909773	1.991502
30	1.639498	1.738112	1.829343	1.9124
40	1.592037	1.692641	1.784519	1.872849
50	1.563033	1.665281	1.75947	1.8478
60	1.544576	1.64547	1.740564	1.830662
70	1.530074	1.631695	1.729147	1.820115
80	1.520511	1.622452	1.7186	1.812204
90	1.5107	1.614449	1.712073	1.802976

observations are true for all boundary conditions.

However, there are some differences in the stability for different boundary conditions. From the value of the critical temperature in the same weight fraction and applied voltage, it could be concluded that the clamped-clamped boundary condition has superior stability over other two supposed BCs.

4.6 Effects of different thickness of piezoelectric layer on critical voltage

In Tables 9-11, variation of weight fraction GNP reinforcement and its effect on the critical voltage of cylindrical shell structure are provided for different values of piezoelectric layer thickness. It is observed that in all thicknesses of the piezoelectric layer, increase in the weight fraction of GNP lead to increase in the critical voltage required for destabilizing the structure. Hence, increase in the weight fraction of GNP has a positive influence of the stability condition of the structure. On the other hand, increase in the thickness of the piezoelectric layer improve the stability through increasing critical voltage. These observations are the case for all boundary conditions. However, there are some differences in the stability for

different boundary conditions. From the value of the critical voltage in the same thickness and weight fraction of the GNP, it could be concluded that the clamped-clamped boundary condition has superior stability over other two supposed BCs.

5. Conclusions

Many of small-scale devices should be designed to tolerate high temperature changes. In the present study, the state of buckling and stability of nano-scale cylindrical shell structure integrated with piezoelectric layer under various thermal and electrical external loadings is scrutinized. In this regard, a multi-layer composite shell reinforced with graphene nano-platelets (GNP) having different patterns of layer configurations is considered. An outer layer of piezoelectric material receiving external voltage is also attached to the cylindrical shell for the aim of observing effects of voltage of the thermal buckling condition. The cylindrical shell is mathematically modeled with first-order shear deformation theory (FSDT). Linear elasticity relationship with constant thermal expansion coefficient is used to extract the relationship between stress and strain components. Moreover, minimum virtual work, including the work of the piezoelectric layer, is engaged to derive equations of motion. The derived equations are solved using numerical method to find out the effects of temperature and external voltage on the buckling stability of the shell structure. It is revealed that:

- The buckling stability condition of cylindrical nanocomposite shell structure is highly dependent on the geometry of piezoelectric layer, applied external voltage, temperature change and weight fraction of GNP.
- Increase in the weight fraction of GNP has a positive influence of the stability condition of the structure.
- Increase in the thickness of the piezoelectric layer improve the stability through increasing critical temperature.
- Increase in the weight fraction of GNP improve the stability through increasing critical temperature change.

Ackknowledgment

This work was supported by Introduction and Education Plan of Young Creative Talents in Universities of Shandong Province（500076).

References

Adamian, A., Safari, K.H., Sheikholeslami, M., Habibi, M., Al-Furjan, M. and Chen, G. (2020), "Critical temperature and frequency characteristics of GPLs-reinforced composite doubly curved panel", *Appl. Sci.*, **10**(9), 3251. https://doi.org/10.3390/app10093251

Al-Furjan, M., Dehini, R., Khorami, M., Habibi, M. and won Jung, D. (2020a), "On the dynamics of the ultra-fast rotating cantilever orthotropic piezoelectric nanodisk based on nonlocal strain gradient theory", *Compos. Struct.*, 112990. https://doi.org/10.1016/j.compstruct.2020.112990

Al-Furjan, M., Fereidouni, M., Habibi, M., Abd Ali, R., Ni, J. and Safarpour, M. (2020b), "Influence of in-plane loading on the vibrations of the fully symmetric mechanical systems via dynamic simulation and generalized differential quadrature framework", *Eng. Comput.*, 1-23. https://doi.org/10.1007/s00366-020-01177-7

Al-Furjan, M., Fereidouni, M., Sedghiyan, D., Habibi, M. and won Jung, D. (2020c), "Three-dimensional frequency response of the CNT-Carbon-Fiber reinforced laminated circular/annular plates under initially stresses", *Compos. Struct.*, 113146. https://doi.org/10.1016/j.compstruct.2020.113146

Al-Furjan, M., Habibi, M., won Jung, D. and Safarpour, H. (2020d), "Vibrational characteristics of a higher-order laminated composite viscoelastic annular microplate via modified couple stress theory", *Compos. Struct.*, 113152. https://doi.org/10.1016/j.compstruct.2020.113152

Al-Furjan, M., Moghadam, S.A., Dehini, R., Shan, L., Habibi, M. and Safarpour, H. (2020e), "Vibration control of a smart shell reinforced by graphene nanoplatelets under external load: Semi-numerical and finite element modeling", 107242. https://doi.org/10.1016/j.tws.2020.107242

Al-Furjan, M., Oyarhossein, M.A., Habibi, M., Safarpour, H. and Jung, D.W. (2020f), "Frequency and critical angular velocity characteristics of rotary laminated cantilever microdisk via two-dimensional analysis", *Thin Wall. Struct.*, **157**, 107111. https://doi.org/10.1016/j.tws.2020.107111

Al-Furjan, M.S.H., Habibi, M., Ebrahimi, F., Mohammadi, K. and Safarpour, H. (2020g), "Wave dispersion characteristics of high-speed-rotating laminated nanocomposite cylindrical shells based on four continuum mechanics theories", *Wave Random Complex Med.*, 1-27. https://doi.org/10.1080/17455030.2020.1831099

Alipour, M., Torabi, M.A., Sareban, M., Lashini, H., Sadeghi, E., Fazaeli, A., Habibi, M. and Hashemi, R. (2020), "Finite element and experimental method for analyzing the effects of martensite morphologies on the formability of DP steels", *Mech Based Des. Struct.*, **48**(5), 525-541. https://doi.org/10.1080/15397734.2019.1633343

Bai, Y., Alzahrani, B., Baharom, S. and Habibi, M. (2020), "Semi-numerical simulation for vibrational responses of the viscoelastic imperfect annular system with honeycomb core under residual pressure", *Eng. Comput.*, 1-26. https://doi.org/10.1007/s00366-020-01191-9

Chen, F., Chen, J., Duan, R., Habibi, M. and Khadimallah, M.A. (2022), "Investigation on dynamic stability and aeroelastic characteristics of composite curved pipes with any yawed angle", *Compos. Struct.*, 115195. https://doi.org/10.1016/j.compstruct.2022.115195

Cheshmeh, E., Karbon, M., Eyvazian, A., Jung, D.w., Habibi, M. and Safarpour, M. (2020), "Buckling and vibration analysis of FG-CNTRC plate subjected to thermo-mechanical load based on higher order shear deformation theory", *Mech Based Des. Struct.*, 1-24. https://doi.org/10.1080/15397734.2020.1744005

Dai, Z., Jiang, Z., Zhang, L. and Habibi, M. (2021a), "Frequency characteristics and sensitivity analysis of a size-dependent laminated nanoshell", *Adv. Nano Res.*, **10**(2), 175. https://doi.org/10.12989/anr.2021.10.2.175

Dai, Z., Tang, H., Wu, S., Habibi, M., Moradi, Z. and Ali, H.E. (2023a), "Nonlinear consecutive dynamic instabilities of thermally shocked composite circular plates on the softening elastic foundation", *Thin Wall. Struct.*, **186**, 110645. https://doi.org/10.1016/j.tws.2023.110645

Dai, Z., Wu, S., Habibi, M. and Ali, H.E. (2023b), "Application of point interpolation mesh-free method for magneto/electro rheological vibrations of sandwich conical panels", *Aerosp. Sci. Technol.*, 108180. https://doi.org/10.1016/j.ast.2023.108180

Dai, Z., Zhang, L., Bolandi, S.Y. and Habibi, M. (2021b), "On the vibrations of the non-polynomial viscoelastic composite open-type shell under residual stresses", *Compos. Struct.*, 113599. https://doi.org/10.1016/j.compstruct.2021.113599

Dong, Y., Gao, Y., Zhu, Q., Moradi, Z. and Safa, M. (2022), "TE-GDQE implementation to investigate the vibration of FG composite conical shells considering a frequency controller solid ring", *Eng. Anal. Bound. Elem.*, **138**, 95-107. https://doi.org/10.1016/j.enganabound.2022.01.017

Du, S., Xie, H., Yin, J., Fang, T., Zhang, S., Sun, Y., Cai, C., Bi, G., Chen, Z. and Xiao, D. (2023), "Competition pathways of energy relaxation of hot electrons through coupling with optical, surface, and acoustic phonons", *J. Phys. Chem. C*, **127**(4), 1929-1936. https://doi.org/10.1021/acs.jpcc.2c07791

Ebrahimi, F., Habibi, M. and Safarpour, H. (2019a), "On modeling of wave propagation in a thermally affected GNP-reinforced imperfect nanocomposite shell", *Eng. Comput.*, **35**(4), 1375-1389. https://doi.org/10.1007/s00366-018-0669-4

Ebrahimi, F., Hajilak, Z.E., Habibi, M. and Safarpour, H. (2019b), "Buckling and vibration characteristics of a carbon nanotube-reinforced spinning cantilever cylindrical 3D shell conveying viscous fluid flow and carrying spring-mass systems under various temperature distributions", *Proceedings of the Institution of Mechanical Engineers, Part C: Journal of Mechanical Engineering Science*, **233**(13), 4590-4605. https://doi.org/10.1177/0954406219832323

Ebrahimi, F., Hashemabadi, D., Habibi, M. and Safarpour, H. (2020a), "Thermal buckling and forced vibration characteristics of a porous GNP reinforced nanocomposite cylindrical shell", *Microsyst. Technol.*, **26**(2), 461-473. https://doi.org/10.1007/s00542-019-04542-9

Ebrahimi, F., Mohammadi, K., Barouti, M.M. and Habibi, M. (2019c), "Wave propagation analysis of a spinning porous graphene nanoplatelet-reinforced nanoshell", *Wave Random Complex Med.*, 1-27. https://doi.org/10.1080/17455030.2019.1694729

Ebrahimi, F., Supeni, E.E.B., Habibi, M. and Safarpour, H. (2020b), "Frequency characteristics of a GPL-reinforced composite microdisk coupled with a piezoelectric layer", *Eur. Phys. J. Plus*, **135**(2), 144. https://doi.org/10.1140/epjp/s13360-020-00217-x

Esmailpoor Hajilak, Z., Pourghader, J., Hashemabadi, D., Sharifi Bagh, F., Habibi, M. and Safarpour, H. (2019), "Multilayer GPLRC composite cylindrical nanoshell using modified strain gradient theory", *Mech Based Des. Struct.*, **47**(5), 521-545. https://doi.org/10.1080/15397734.2019.1566743

Fan, L., Huang, Y., Ji, D., Moradi, Z., Safa, M. and Amine Khadimallah, M. (2022), "Interaction of angular velocity and temperature rise in the thermo-inertia bifurcation buckling of FG laminated nanocomposite annular plates", *Eng. Struct.*, **265**, 114518. https://doi.org/10.1016/j.engstruct.2022.114518

Fu, Y., Pan, Q., Liu, G. and Zhang, G. (2023), "Gradient structure of Ti-55531 with nano-ultrafine grains fabricated by simulation and suction casting", *J. Mater. Eng. Perform.*, **32**(7), 3084-3093.

Ghadiri, M. and Safarpour, H. (2016), "Free vibration analysis of embedded magneto-electro-thermo-elastic cylindrical nanoshell based on the modified couple stress theory", *Appl. Phys. A*, **122**(9), 833. https://doi.org/10.1007/s00339-016-0365-4

Ghazanfari, A., Soleimani, S.S., Keshavarzzadeh, M., Habibi, M., Assempuor, A. and Hashemi, R. (2020), "Prediction of FLD for sheet metal by considering through-thickness shear stresses", *Mech Based Des. Struct.*, **48**(6), 755-772. https://doi.org/10.1080/15397734.2019.1662310

Gong, S., Sheng, X., Li, X., Sheng, M., Wu, H., Lu, X. and Qu, J. (2022), "A multifunctional flexible composite film with excellent multi-source driven thermal management, electromagnetic interference shielding, and fire safety performance, inspired by a "brick–mortar" sandwich structure", *Adv. Funct. Mater.*, 2200570. https://doi.org/10.1002/adfm.202200570

Gu, M., Mo, H., Qiu, J., Yuan, J. and Xia, Q. "Behavior of floating stone columns reinforced with geogrid encasement in model tests", *Front. Mater.*, 503. https://doi.org/10.3389/fmats.2022.980851

Guan, H., Huang, S., Ding, J., Tian, F., Xu, Q. and Zhao, J. (2020), "Chemical environment and magnetic moment effects on point defect formations in CoCrNi-based concentrated solid-solution alloys", *Acta Materialia*. **187**, 122-134. https://doi.org/10.1016/j.actamat.2020.01.044

Guo, J., Baharvand, A., Tazeddinova, D., Habibi, M., Safarpour, H., Roco-Videla, A. and Selmi, A. (2021a), "An intelligent computer method for vibration responses of the spinning multi-layer symmetric nanosystem using multi-physics modeling", *Eng. Comput.*, 1-22. https://doi.org/10.1007/s00366-021-01433-4

Guo, Y., Mi, H. and Habibi, M. (2021b), "Electromechanical energy absorption, resonance frequency, and low-velocity impact analysis of the piezoelectric doubly curved system", *Mech. Syst. Signal Pr.*, **157**, 107723. https://doi.org/10.1016/j.ymssp.2021.107723

Habibi, M., Darabi, R., Sa, J.C.d. and Reis, A. (2021), "An innovation in finite element simulation via crystal plasticity assessment of grain morphology effect on sheet metal formability", *Proceedings of the Institution of Mechanical Engineers, Part L: Journal of Materials: Design and Applications*. **235**(8), 1937-1951. https://doi.org/10.1177/14644207211024686

Habibi, M., Ghazanfari, A., Assempour, A., Naghdabadi, R. and Hashemi, R. (2017), "Determination of forming limit diagram using two modified finite element models", *Mech. Eng.*, **48**(4), 141-144. https://doi.org/10.22060/MEJ.2016.664

Habibi, M., Hashemabadi, D. and Safarpour, H. (2019a), "Vibration analysis of a high-speed rotating GPLRC nano-structure coupled with a piezoelectric actuator", *Eur. Phys. J. Plus*, **134**(6), 307.

Habibi, M., Hashemi, R., Ghazanfari, A., Naghdabadi, R. and Assempour, A. (2018a), "Forming limit diagrams by including the M–K model in finite element simulation considering the effect of bending", *Proceedings of the Institution of Mechanical Engineers, Part L: Journal of Materials: Design and Applications*, **232**(8), 625-636.

Habibi, M., Hashemi, R., Sadeghi, E., Fazaeli, A., Ghazanfari, A. and Lashini, H. (2016), "Enhancing the mechanical properties and formability of low carbon steel with dual-phase micro-structures", *J. Mater. Eng. Perform.*, **25**(2), 382-389.

Habibi, M., Hashemi, R., Tafti, M.F. and Assempour, A. (2018b), "Experimental investigation of mechanical properties, formability and forming limit diagrams for tailor-welded blanks produced by friction stir welding", *J. Manuf. Proc.*, **31**, 310-323. https://doi.org/10.1016/j.jmapro.2017.11.009

Habibi, M., Mohammadgholiha, M. and Safarpour, H. (2019b), "Wave propagation characteristics of the electrically GNP-reinforced nanocomposite cylindrical shell", *J. Brazil. Soc. Mech. Sci. Eng.*, **41**(5), 221.

Habibi, M., Mohammadi, A., Safarpour, H., Shavalipour, A. and Ghadiri, M. (2019c), "Wave propagation analysis of the laminated cylindrical nanoshell coupled with a piezoelectric actuator", *Mech Based Des. Struct.*, 1-19. https://doi.org/10.1080/15397734.2019.1697932

Habibi, M., Safarpour, M. and Safarpour, H. (2020), "Vibrational characteristics of a FG-GPLRC viscoelastic thick annular plate using fourth-order Runge-Kutta and GDQ methods", *Mech Based Des. Struct.*, 1-22.

https://doi.org/10.1080/15397734.2020.1779086
Habibi, M., Taghdir, A. and Safarpour, H. (2019d), "Stability analysis of an electrically cylindrical nanoshell reinforced with graphene nanoplatelets", *Compos. Part B Eng*., **175**, 107125. https://doi.org/10.1016/j.compositesb.2019.107125
Hashemi, H.R., Alizadeh, A.A., Oyarhossein, M.A., Shavalipour, A., Makkiabadi, M. and Habibi, M. (2019), "Influence of imperfection on amplitude and resonance frequency of a reinforcement compositionally graded nanostructure", *Wave Random Complex Med*., 1-27. https://doi.org/10.1080/17455030.2019.1662968
He, X., Ding, J., Habibi, M., Safarpour, H. and Safarpour, M. (2021), "Non-polynomial framework for bending responses of the multi-scale hybrid laminated nanocomposite reinforced circular/annular plate", *Thin Wall. Struct*., **166**, 108019. https://doi.org/10.1016/j.tws.2021.108019
Hou, F., Wu, S., Moradi, Z. and Shafiei, N. (2021a), "The computational modeling for the static analysis of axially functionally graded micro-cylindrical imperfect beam applying the computer simulation", *Eng. Comput.*, 1-19.
Hou, F., Wu, S., Moradi, Z. and Shafiei, N. (2021b), "The computational modeling for the static analysis of axially functionally graded micro-cylindrical imperfect beam applying the computer simulation", *Eng. Comput*., **38**(Suppl 4), 3217-3235. https://doi.org/10.1007/s00366-021-01456-x
Huang, X., Cao, M., Wang, D., Li, X., Fan, J. and Li, X. (2022), "Broadband polarization-insensitive and oblique-incidence terahertz metamaterial absorber with multi-layered graphene", *Opt. Mater. Exp*., **12**(2), 811-822. https://doi.org/10.1364/OME.451450
Huang, X., Hao, H., Oslub, K., Habibi, M. and Tounsi, A. (2021a), "Dynamic stability/instability simulation of the rotary size-dependent functionally graded microsystem", *Eng. Comput*., 1-17. https://doi.org/10.1007/s00366-021-01399-3
Huang, X., Zhang, Y., Moradi, Z. and Shafiei, N. (2021b), "Computer simulation via a couple of homotopy perturbation methods and the generalized differential quadrature method for nonlinear vibration of functionally graded non-uniform micro-tube", *Eng. Comput*., 1-18. https://doi.org/10.1007/s00366-021-01395-7
Huang, X., Zhu, Y., Vafaei, P., Moradi, Z. and Davoudi, M. (2021c), "An iterative simulation algorithm for large oscillation of the applicable 2D-electrical system on a complex nonlinear substrate", *Eng. Comput*., 1-13. https://doi.org/10.1007/s00366-021-01320-y
Ji, B., Zhang, F., Song, X. and Tang, Y. (2017), "A novel potassium-ion-based dual-ion battery", *Adv. Mater*., **29**(19), 1700519. https://doi.org/10.1002/adma.201700519
Jiao, J., Ghoreishi, S.M., Moradi, Z. and Oslub, K. (2021), "Coupled particle swarm optimization method with genetic algorithm for the static–dynamic performance of the magneto-electro-elastic nanosystem", *Eng. Comput*., 1-15. https://doi.org/10.1007/s00366-021-01391-x
Ke, L., Wang, Y. and Reddy, J. (2014), "Thermo-electro-mechanical vibration of size-dependent piezoelectric cylindrical nanoshells under various boundary conditions", *Compos. Struct*., **116**, 626-636. https://doi.org/10.1016/j.compstruct.2014.05.048
Khalili, S. and Mohammadi, Y. (2012), "Free vibration analysis of sandwich plates with functionally graded face sheets and temperature-dependent material properties: A new approach", *Eur. J. Mech. A Solids*, **35**, 61-74. https://doi.org/10.1016/j.euromechsol.2012.01.003
Kong, F., Dong, F., Duan, M., Habibi, M., Safarpour, H. and Tounsi, A. (2022), "On the vibrations of the Electrorheological sandwich disk with composite face sheets considering pre and post-yield regions", *Thin Wall. Struct*., **179**, 109631. https://doi.org/10.1016/j.tws.2022.109631
Li, J., Tang, F. and Habibi, M. (2020a), "Bi-directional thermal buckling and resonance frequency characteristics of a GNP-reinforced composite nanostructure", *Eng. Comput*., 1-22. https://doi.org/10.1007/s00366-020-01110-y
Li, Y., Li, S., Guo, K., Fang, X. and Habibi, M. (2020b), "On the modeling of bending responses of graphene-reinforced higher order annular plate via two-dimensional continuum mechanics approach", *Eng. Comput*., 1-22. https://doi.org/10.1007/s00366-020-01166-w
Liu, H., Shen, S., Oslub, K., Habibi, M. and Safarpour, H. (2021a), "Amplitude motion and frequency simulation of a composite viscoelastic microsystem within modified couple stress elasticity", *Eng. Comput*., 1-15. https://doi.org/10.1007/s00366-021-01316-8
Liu, H., Zhao, Y., Pishbin, M., Habibi, M., Bashir, M. and Issakhov, A. (2021b), "A comprehensive mathematical simulation of the composite size-dependent rotary 3D microsystem via two-dimensional generalized differential quadrature method", *Eng. Comput*., 1-16. https://doi.org/10.1007/s00366-021-01419-2
Liu, Y., Wang, W., He, T., Moradi, Z. and Larco Benítez, M.A. (2021c), "On the modelling of the vibration behaviors via discrete singular convolution method for a high-order sector annular system", *Eng. Comput*., 1-23.
Liu, Z., Su, S., Xi, D. and Habibi, M. (2020a), "Vibrational responses of a MHC viscoelastic thick annular plate in thermal environment using GDQ method", *Mech Based Des. Struct*., 1-26. https://doi.org/10.1080/15397734.2020.1784201
Liu, Z., Wu, X., Yu, M. and Habibi, M. (2020b), "Large-amplitude dynamical behavior of multilayer graphene platelets reinforced nanocomposite annular plate under thermo-mechanical loadings", *Mech Based Des. Struct*., 1-25. https://doi.org/10.1080/15397734.2020.1815544
Lori, E.S., Ebrahimi, F., Supeni, E.E.B., Habibi, M. and Safarpour, H. (2020), "The critical voltage of a GPL-reinforced composite microdisk covered with piezoelectric layer", *Eng. Comput*., 1-20. https://doi.org/10.1007/s00366-020-01004-z
Lu, C., Zhu, R., Yu, F., Jiang, X., Liu, Z., Dong, L., Hua, Q. and Ou, Z. (2021), "Gear rotational speed sensor based on FeCoSiB/Pb (Zr, Ti) O3 magnetoelectric composite", *Measurement*. **168** 108409. https://doi.org/10.1016/j.measurement.2020.108409
Luo, J., Song, J., Moradi, Z., Safa, M. and Khadimallah, M.A. (2022a), "Effect of simultaneous compressive and inertia loads on the bifurcation stability of shear deformable functionally graded annular fabrications reinforced with graphenes", *Eur. J. Mech. A Solids*, 104581. https://doi.org/10.1016/j.euromechsol.2022.104581
Luo, J., Wu, S., Hou, S., Moradi, Z., Habibi, M. and Khadimallah, M.A. (2022b), "Thermally nonlinear thermoelasticity of a one-dimensional finite domain based on the finite strain concept", *Eur. J. Mech. A Solids*, 104726. https://doi.org/10.1016/j.euromechsol.2022.104726
Ma, L., Liu, X. and Moradi, Z. "On the chaotic behavior of graphene-reinforced annular systems under harmonic excitation", *Eng. Comput*., 1-25. https://doi.org/10.1007/s00366-020-01210-9
Ma, L., Liu, X. and Moradi, Z. (2021), "On the chaotic behavior of graphene-reinforced annular systems under harmonic excitation", *Eng. Comput*., 1-25. https://doi.org/10.1007/s00366-020-01210-9
Michael, M., Meyyazhagan, A., Velayudhannair, K., Pappuswamy, M., Maria, A., Xavier, V., Balasubramanian, B., Baskaran, R., Kamyab, H. and Vasseghian, Y. (2022), "The content of heavy metals in cigarettes and the impact of their leachates on the aquatic ecosystem", *Sustainability*. **14**(8), 4752.

https://doi.org/10.3390/su14084752

Moayedi, H., Aliakbarlou, H., Jebeli, M., Noormohammadiarani, O., Habibi, M., Safarpour, H. and Foong, L. (2020a), "Thermal buckling responses of a graphene reinforced composite micropanel structure", *Int. J. Appl. Mech.*, **12**(1), 2050010. https://doi.org/10.1142/S1758825120500106

Moayedi, H., Ebrahimi, F., Habibi, M., Safarpour, H. and Foong, L.K. (2020b), "Application of nonlocal strain–stress gradient theory and GDQEM for thermo-vibration responses of a laminated composite nanoshell", *Eng. Comput.*, 1-16. https://doi.org/10.1007/s00366-020-01002-1

Moayedi, H., Habibi, M., Safarpour, H., Safarpour, M. and Foong, L. (2019), "Buckling and frequency responses of a graphene nanoplatelet reinforced composite microdisk", *Int. J. Appl. Mech.*, **11**(10), 1950102. https://doi.org/10.1142/S1758825119501023

Mohammadgholiha, M., Shokrgozar, A., Habibi, M. and Safarpour, H. (2019), "Buckling and frequency analysis of the nonlocal strain–stress gradient shell reinforced with graphene nanoplatelets", *J. Vib. Control*, **25**(19-20), 2627-2640. https://doi.org/10.1177/1077546319863251

Mohammadi, A., Lashini, H., Habibi, M. and Safarpour, H. (2019), "Influence of viscoelastic foundation on dynamic behaviour of the double walled cylindrical inhomogeneous micro shell using MCST and with the aid of GDQM", *J. Solid Mech.*, **11**(2), 440-453. https://doi.org/10.22034/jsm.2019.665264

Moradi, Z., Davoudi, M., Ebrahimi, F. and Ehyaei, A.F. (2021), "Intelligent wave dispersion control of an inhomogeneous micro-shell using a proportional-derivative smart controller", *Wave Random Complex Med.*, 1-24. https://doi.org/10.1080/17455030.2021.1926572

Najaafi, N., Jamali, M., Habibi, M., Sadeghi, S., Jung, D.w. and Nabipour, N. (2020), "Dynamic instability responses of the substructure living biological cells in the cytoplasm environment using stress-strain size-dependent theory", *J. Biomol. Struct. Dyn.*, 1-12. https://doi.org/10.1080/07391102.2020.1751297

Nasihatgozar, M. and Khalili, S. (2017), "Free vibration of a thick sandwich plate using higher order shear deformation theory and DQM for different boundary conditions", *J. Appl. Comput. Mech.*, **3**(1), 16-24. https://doi.org/10.22055/jacm.2017.12548

Ning, F., He, G., Sheng, C., He, H., Wang, J., Zhou, R. and Ning, X. (2021), "Yarn on yarn abrasion performance of high modulus polyethylene fiber improved by graphene/polyurethane composites coating", *J. Eng. Fibers Fab.*, **16**, 1558925020983563. https://doi.org/10.1177/1558925020983563

Oyarhossein, M.A., Alizadeh, A.a., Habibi, M., Makkiabadi, M., Daman, M., Safarpour, H. and Jung, D.W. (2020), "Dynamic response of the nonlocal strain-stress gradient in laminated polymer composites microtubes", *Sci. Rep.*, **10**(1), 1-19. https://doi.org/10.1038/s41598-020-61855-w

Peng, S., Habibi, M. and Pourjabari, A. (2023), "Generalized differential quadrature element solution, swarm, and GA optimization technique to obtain the optimum frequency of the laminated rotary nanostructure", *Eng. Anal. Bound. Elem.*, **151**, 101-114. https://doi.org/10.1016/j.enganabound.2023.02.052

Pourjabari, A., Hajilak, Z.E., Mohammadi, A., Habibi, M. and Safarpour, H. (2019), "Effect of porosity on free and forced vibration characteristics of the GPL reinforcement composite nanostructures", *Comput. Math. Appl.*, **77**(10), 2608-2626.

Pourmoayed, A., Fard, K.M. and Shahravi, M. (2017), "Vibration analysis of a cylindrical sandwich panel with flexible core using an improved higher-order theory", *Latin Am. J. Solid Struct.*, **14**(4), 714-742. https://doi.org/10.1590/1679-78253410

Rajasekaran, S. (2009), *Structural Dynamics of Earthquake Engineering: Theory and Application Using MATHEMATICA and MATLAB*, Elsevier.

Ren, R., Lai, F., Lang, X., Li, L., Yao, C. and Cai, K. (2023), "Efficient sulfur host based on Sn doping to construct Fe2O3 nanospheres with high active interface structure for lithium-sulfur batteries", *Appl. Surf. Sci.*, **613**, 156003. https://doi.org/10.1016/j.apsusc.2022.156003.

Sabzevari, F., Amelirad, O., Moradi, Z. and Habibi, M. (2023), "Artificial intelligence evaluation of COVID-19 restrictions and speech therapy effects on the autistic children's behavior", *Sci. Rep.*, **13**(1), 4312. https://doi.org/10.1038/s41598-022-25902-y

Safarpour, H., Ali Ghanizadeh, S. and Habibi, M. (2018a), "Wave propagation characteristics of a cylindrical laminated composite nanoshell in thermal environment based on the nonlocal strain gradient theory", *Eur. Phys. J. Plus.* **133**(12), 532. https://doi.org/10.1140/epjp/i2018-12385-2

Safarpour, H., Ghanizadeh, S.A. and Habibi, M. (2018b), "Wave propagation characteristics of a cylindrical laminated composite nanoshell in thermal environment based on the nonlocal strain gradient theory", *Eur. Phys. J. Plus*, **133**(12), 532.

Safarpour, H., Hajilak, Z.E. and Habibi, M. (2019a), "A size-dependent exact theory for thermal buckling, free and forced vibration analysis of temperature dependent FG multilayer GPLRC composite nanostructures restring on elastic foundation", *Int. J. Mech. Mater. Des.*, **15**(3), 569-583. https://doi.org/10.1007/s10999-018-9431-8

Safarpour, H., Pourghader, J. and Habibi, M. (2019b), "Influence of spring-mass systems on frequency behavior and critical voltage of a high-speed rotating cantilever cylindrical three-dimensional shell coupled with piezoelectric actuator", *J. Vib. Control*, **25**(9), 1543-1557. https://doi.org/10.1177/1077546319828465

Safarpour, M., Ebrahimi, F., Habibi, M. and Safarpour, H. (2020), "On the nonlinear dynamics of a multi-scale hybrid nanocomposite disk", *Eng. Comput.*, 1-20. https://doi.org/10.1007/s00366-020-00949-5

Shao, Y., Zhao, Y., Gao, J. and Habibi, M. (2021), "Energy absorption of the strengthened viscoelastic multi-curved composite panel under friction force", *Arch. Civil Mech. Eng.*, **21**(4), 1-29. https://doi.org/10.1007/s43452-021-00279-3

Shariati, A., Habibi, M., Tounsi, A., Safarpour, H. and Safa, M. (2020a), "Application of exact continuum size-dependent theory for stability and frequency analysis of a curved cantilevered microtubule by considering viscoelastic properties", *Eng. Comput.*, 1-20. https://doi.org/10.1007/s00366-020-01024-9

Shariati, A., Mohammad-Sedighi, H., Żur, K.K., Habibi, M. and Safa, M. (2020b), "On the vibrations and stability of moving viscoelastic axially functionally graded nanobeams", *Materials*, **13**(7), 1707. https://doi.org/10.3390/ma13071707

Shariati, A., Mohammad-Sedighi, H., Żur, K.K., Habibi, M. and Safa, M. (2020c), "Stability and dynamics of viscoelastic moving rayleigh beams with an asymmetrical distribution of material parameters", *Symmetry*, **12**(4), 586. https://doi.org/10.3390/sym12040586

Shariati, M., Azar, S.M., Arjomand, M.-A., Tehrani, H.S., Daei, M. and Safa, M. (2020d), "Evaluating the impacts of using piles and geosynthetics in reducing the settlement of fine-grained soils under static load", *Geomech. Eng.*, **20**(2), 87-101. https://doi.org/10.12989/gae.2020.20.2.087

Shariati, M., Davoodnabi, S.M., Toghroli, A., Kong, Z. and Shariati, A. (2021a), "Hybridization of metaheuristic algorithms with adaptive neuro-fuzzy inference system to predict load-slip behavior of angle shear connectors at elevated temperatures", *Compos. Struct.*, 114524. https://doi.org/10.1016/j.compstruct.2021.114524

Shariati, M., Faegh, S.S., Mehrabi, P., Bahavarnia, S., Zandi, Y., Masoom, D.R., Toghroli, A., Trung, N.T. and Salih, M.N. (2019), "Numerical study on the structural performance of corrugated low yield point steel plate shear walls with circular

openings", *Steel Compos. Struct.*, **33**(4), 569-581. https://doi.org/10.12989/scs.2019.33.4.569

Shariati, M., Ghorbani, M., Naghipour, M., Alinejad, N. and Toghroli, A. (2020e), "The effect of RBS connection on energy absorption in tall buildings with braced tube frame system", *Steel Compos. Struct.*, **34**(3), 393-407. https://doi.org/10.12989/scs.2020.34.3.393

Shariati, M., Kamyab, H., Habibi, M., Ahmadi, S., Naghipour, M., Gorjinezhad, F., Mohammadirad, S. and Aminian, A. (2023), "Sulfuric acid resistance of concrete containing coal waste as a partial substitute for fine and coarse aggregates", *Fuel*, **348**, 128311. https://doi.org/10.1016/j.fuel.2023.128311

Shariati, M., Lagzian, M., Maleki, S., Shariati, A. and Trung, N.T. (2020f), "Evaluation of seismic performance factors for tension-only braced frames", *Steel Compos. Struct.*, **35**(4), 599-609. https://doi.org/10.12989/scs.2020.35.4.599

Shariati, M., Mafipour, M.S., Ghahremani, B., Azarhomayun, F., Ahmadi, M., Trung, N.T. and Shariati, A. (2020g), "A novel hybrid extreme learning machine–grey wolf optimizer (ELM-GWO) model to predict compressive strength of concrete with partial replacements for cement", *Eng. Comput.*, 1-23. https://doi.org/10.1007/s00366-020-01081-0

Shariati, M., Mafipour, M.S., Mehrabi, P., Ahmadi, M., Wakil, K., Trung, N.T. and Toghroli, A. (2020h), "Prediction of concrete strength in presence of furnace slag and fly ash using Hybrid ANN-GA (Artificial Neural Network-Genetic Algorithm)", *Smart Struct. Syst.*, **25**(2), 183-195. https://doi.org/10.12989/sss.2020.25.2.183

Shariati, M., Naghipour, M., Yousofizinsaz, G., Toghroli, A. and Tabarestani, N.P. (2020i), "Numerical study on the axial compressive behavior of built-up CFT columns considering different welding lines", *Steel Compos. Struct.* **34**(3), 377-391. http://dx.doi.org/10.12989/scs.2020.34.3.377

Shariati, M., Shariati, A., Trung, N.T., Shoaei, P., Ameri, F., Bahrami, N. and Zamanabadi, S.N. (2021b), "Alkali-activated slag (AAS) paste: Correlation between durability and microstructural characteristics", *Constr. Build. Mater.*, **267**, 120886. https://doi.org/10.1016/j.conbuildmat.2020.120886

Shariati, M., Sulong, N.R. and Khanouki, M.A. (2012), "Experimental assessment of channel shear connectors under monotonic and fully reversed cyclic loading in high strength concrete", *Mater. Des.*, **34**, 325-331. https://doi.org/10.1016/j.matdes.2011.08.008

Shariati, M., Sulong, N.R., Shariati, A. and Khanouki, M.A. (2016a), "Behavior of V-shaped angle shear connectors: Experimental and parametric study", *Mater. Struct.*, **49**(9), 3909-3926. https://doi.org/10.1617/s11527-015-0762-8

Shariati, M., Sulong, N.R., Shariati, A. and Kueh, A. (2016b), "Comparative performance of channel and angle shear connectors in high strength concrete composites: An experimental study", *Constr. Build. Mater.*, **120**, 382-392. https://doi.org/10.1016/j.conbuildmat.2016.05.102

Shariati, M., Tahmasbi, F., Mehrabi, P., Bahadori, A. and Toghroli, A. (2020j), "Monotonic behavior of C and L shaped angle shear connectors within steel-concrete composite beams: An experimental investigation", *Steel Compos Struct.* **35**(2), 237-247. http://doi.org/10.12989/scs.2020.35.2.237

Sheng, C., He, G., Hu, Z., Chou, C., Shi, J., Li, J., Meng, Q., Ning, X., Wang, L. and Ning, F. (2021), "Yarn on yarn abrasion failure mechanism of ultrahigh molecular weight polyethylene fiber", *J. Eng. Fibers Fabr.*, **16**, 15589250211052766. https://doi.org/10.1177/15589250211052766

Shi, Y., Guo, Z., Zhu, D., Pan, J. and Lu, S. (2023), "Isothermal reduction kinetics and microstructure evolution of various vanadium titanomagnetite pellets in direct reduction", *J. Alloys Compd.*, **953**, 170126.

Shokrgozar, A., Safarpour, H. and Habibi, M. (2020), "Influence of system parameters on buckling and frequency analysis of a spinning cantilever cylindrical 3D shell coupled with piezoelectric actuator", *Proceedings of the Institution of Mechanical Engineers, Part C: Journal of Mechanical Engineering Science*, **234**(2), 512-529. https://doi.org/10.1177/0954406219883312

Song, M., Kitipornchai, S. and Yang, J. (2017), "Free and forced vibrations of functionally graded polymer composite plates reinforced with graphene nanoplatelets", *Compos. Struct.*, **159**, 579-588. https://doi.org/10.1016/j.compstruct.2016.09.070

Sun, N., Yao, X., Liu, J., Li, J., Yang, N., Zhao, G. and Dai, C. (2023), "Breakup and coalescence mechanism of high-stability bubbles reinforced by dispersed particle gel particles in the pore-throat micromodel", *Geoenerg Sci. Eng.*, **223**, 211513. https://doi.org/10.1016/j.geoen.2023.211513.

Tong, X., Zhang, F., Ji, B., Sheng, M. and Tang, Y. (2016), "Carbon-coated porous aluminum foil anode for high-rate, long-term cycling stability, and high energy density dual-ion batteries", *Adv. Mater.*, **28**(45), 9979-9985. https://doi.org/10.1002/adma.201603735

Wang, H., Habibi, M., Marzouki, R., Majdi, A., Shariati, M., Denic, N., Zakić, A., Khorami, M., Khadimallah, M.A. and Ebid, A.A.K. (2022a), "Improving the self-healing of cementitious materials with a hydrogel system", *Gels.* **8**(5), 278. https://doi.org/10.3390/gels8050278

Wang, M., Jiang, C., Zhang, S., Song, X., Tang, Y. and Cheng, H.-M. (2018), "Reversible calcium alloying enables a practical room-temperature rechargeable calcium-ion battery with a high discharge voltage", *Nature Chem.*, **10**(6), 667-672. https://doi.org/10.1038/s41557-018-0045-4

Wang, P., Gao, Z., Pan, F., Moradi, Z., Mahmoudi, T. and Khadimallah, M.A. (2022b), "A couple of GDQM and iteration techniques for the linear and nonlinear buckling of bi-directional functionally graded nanotubes based on the nonlocal strain gradient theory and high-order beam theory", *Eng. Anal. Bound. Elem.*, **143**, 124-136. https://doi.org/10.1016/j.enganabound.2022.06.007

Wang, Q. (2002), "On buckling of column structures with a pair of piezoelectric layers", *Eng. Struct.*, **24**(2), 199-205. https://doi.org/10.1016/S0141-0296(01)00088-8

Wang, Q., Zhou, G.Y. and Lin, K.C. (2006), "Scale effect on wave propagation of double-walled carbon nanotubes", *Int. J. Solids Struct.*, **43**(20), 6071-6084. https://doi.org/10.12989/cac.2020.25.2.133

Wang, Y., Yang, J., Moradi, Z., Safa, M. and Khadimallah, M.A. (2022c), "Nonlinear dynamic analysis of thermally deformed beams subjected to uniform loading resting on nonlinear viscoelastic foundation", *Eur. J. Mech. A Solids*, **95**, 104638. https://doi.org/10.1016/j.euromechsol.2022.104638

Wang, Z., Yu, S., Xiao, Z. and Habibi, M. (2020), "Frequency and buckling responses of a high-speed rotating fiber metal laminated cantilevered microdisk", *Mech. Adv. Mater. Struct.*, 1-14. https://doi.org/10.1080/15376494.2020.1824284

Wei, Y., Chen, C., Tan, C., He, L., Ren, Z., Zhang, C., Peng, S., Han, J., Zhou, H. and Wang, J. (2022), "High-performance visible to near-infrared broadband Bi2O2Se nanoribbon photodetectors", *Adv. Opt. Mater.*, **10**(23), 2201396. https://doi.org/10.1002/adom.202201396

Wu, H., Kitipornchai, S. and Yang, J. (2017), "Thermal buckling and postbuckling of functionally graded graphene nanocomposite plates", *Mater. Des.*, **132**, 430-441. https://doi.org/10.1016/j.matdes.2017.07.025

Wu, J. and Habibi, M. (2021), "Dynamic simulation of the ultra-fast-rotating sandwich cantilever disk via finite element and semi-numerical methods", *Eng. Comput.*, 1-17. https://doi.org/10.1007/s00366-021-01396-6

Wu, Y., Zhao, Y., Han, X., Jiang, G., Shi, J., Liu, P., Khan, M.Z.,

Huhtinen, H., Zhu, J. and Jin, Z. (2021), "Ultra-fast growth of cuprate superconducting films: dual-phase liquid assisted epitaxy and strong flux pinning", *Mater. Today Phys.*, **18**, 100400. https://doi.org/10.1016/j.mtphys.2021.100400

Xia, W., Du, J., Habibi, M., Shariati, M. and Khadimallah, M.A. (2022), "Application of Chebyshev-based GDQ and Newmark methods to viscothermoelasticity responses of FG composite annular systems", *Eng. Anal. Bound. Elem.*, **143**, 28-42. https://doi.org/10.1016/j.enganabound.2022.06.003

Xiang, J., Lai, Y., Moradi, Z. and Khorami, M. (2023), "Wave propagation phenomenon of functionally graded graphene oxide powder-strengthened nanocomposite curved beam", *Solid State Commun.*, 115193. https://doi.org/10.1016/j.ssc.2023.115193

Xiong, Q.M., Chen, Z., Huang, J.T., Zhang, M., Song, H., Hou, X.F., Li, X.B. and Feng, Z.J. (2020), "Preparation, structure and mechanical properties of Sialon ceramics by transition metal-catalyzed nitriding reaction", *Rare Metals*, **39**(5), 589-596. https://doi.org/10.1007/s12598-020-01385-6.

Xu, W., Pan, G., Moradi, Z. and Shafiei, N. (2021a), "Nonlinear forced vibration analysis of functionally graded non-uniform cylindrical microbeams applying the semi-analytical solution", *Compos. Struct.*, 114395. https://doi.org/10.1016/j.compstruct.2021.114395

Xu, W., Pan, G., Moradi, Z. and Shafiei, N. (2021b), "Nonlinear forced vibration analysis of functionally graded non-uniform cylindrical microbeams applying the semi-analytical solution", *Compos. Struct.*, **275**, 114395. https://doi.org/10.1016/j.compstruct.2021.114395

Xu, Y., Chen, X., Zhang, H., Yang, F., Tong, L., Yang, Y., Yan, D., Yang, A., Yu, M. and Liu, Z. "Online identification of battery model parameters and joint state of charge and state of health estimation using dual particle filter algorithms", *Int. J. Energ. Res.*, **46**(14), 19615-19652. https://doi.org/10.1002/er.8541

Yang, C., Su, C., Hu, H., Habibi, M., Safarpour, H. and Khadimallah, M.A. (2023), "Performance optimization of photovoltaic and solar cells via a hybrid and efficient chimp algorithm", *Solar Energy*, **253**, 343-359. https://doi.org/10.1016/j.solener.2023.02.036

Yang, N., Moradi, Z., Arvin, H., Muhsen, S. and Khadimallah, M.A. (2022a), "A study on small scale thermal dynamic instability of rotating GPL-reinforced microbeams under principal parametric resonance stimulation of axial and transversal modes regarding the proportional damping", *Thin Wall. Struct.*, **180**, 109806. https://doi.org/10.1016/j.tws.2022.109806

Yang, N., Moradi, Z., Khadimallah, M.A. and Arvin, H. (2022b), "Application of the Chebyshev–Ritz route in determination of the dynamic instability region boundary for rotating nanocomposite beams reinforced with graphene platelet subjected to a temperature increment", *Eng. Anal. Bound. Elem.*, **139**, 169-179. https://doi.org/10.1016/j.enganabound.2022.03.013

Yang, S.T., Li, X.Y., Yu, T.L., Wang, J., Fang, H., Nie, F., He, B., Zhao, L., Lü, W.M. and Yan, S.S. (2022c), "High-performance neuromorphic computing based on ferroelectric synapses with excellent conductance linearity and symmetry", *Adv. Funct. Mater.*, **32**(35), 2202366.

Yang, Y., Wang, Y., Zheng, C., Lin, H., Xu, R., Zhu, H., Bao, L. and Xu, X. (2022d), "Lanthanum carbonate grafted ZSM-5 for superior phosphate uptake: Investigation of the growth and adsorption mechanism", *Chem. Eng. J.*, **430**, 133166. https://doi.org/10.1016/j.cej.2021.133166

Yu, X., Maalla, A. and Moradi, Z. (2022), "Electroelastic high-order computational continuum strategy for critical voltage and frequency of piezoelectric NEMS via modified multi-physical couple stress theory", *Mech. Syst. Signal Pr.*, **165**, 108373.

Zare, R., Najaafi, N., Habibi, M., Ebrahimi, F. and Safarpour, H. (2020), "Influence of imperfection on the smart control frequency characteristics of a cylindrical sensor-actuator GPLRC cylindrical shell using a proportional-derivative smart controller", *Smart Struct. Syst.*, **26**(4), 469-480. https://doi.org/10.12989/sss.2020.26.4.469

Zhang, H., Xiao, Y., Xu, Z., Yang, M., Zhang, L., Yin, L., Chai, S., Wang, G., Zhang, L. and Cai, X. (2022a), "Effects of Ni-decorated reduced graphene oxide nanosheets on the microstructural evolution and mechanical properties of Sn-3.0 Ag-0.5 Cu composite solders", *Intermetallics*, **150**, 107683. https://doi.org/10.1016/j.intermet.2022.107683.

Zhang, Q., Liu, Z., Jiang, X., Peng, Y., Zhu, C. and Li, Z. (2022b), "Experimental investigation on performance improvement of cantilever piezoelectric energy harvesters via escapement mechanism from extremely Low-Frequency excitations", *Sust. Energ. Technol. Assess.*, **53**, 102591.

Zhang, Q., Xin, C., Shen, F., Gong, Y., Zi, Y., Guo, H., Li, Z., Peng, Y., Zhang, Q. and Wang, Z.L. (2022c), "Human body IoT systems based on triboelectrification effect: energy harvesting, sensing, interfacing and communication", *Energy Environ. Sci.*, 2022, 9. https://doi.org/10.1039/D2EE01590K

Zhang, S., Lai, Y., Chen, K., Habibi, M., Khorami, M. and Haider Mussa, Z. (2023), "Influence of MWCNT's waviness and aggregation factors on wave dispersion response of MWCNT-strengthened nanocomposite curved beam", *Structures*, **53**, 1239-1249. https://doi.org/10.1016/j.istruc.2023.04.024

Zhang, X., Tang, Y., Zhang, F. and Lee, C.S. (2016), "A novel aluminum–graphite dual-ion battery", *Adv. Energy Mater.*, **6**(11), 1502588. https://doi.org/10.1002/aenm.201502588

Zhang, Y., Wang, Z., Tazeddinova, D., Ebrahimi, F., Habibi, M. and Safarpour, H. (2021), "Enhancing active vibration control performances in a smart rotary sandwich thick nanostructure conveying viscous fluid flow by a PD controller", *Wave Random Complex Med.*, 1-24. https://doi.org/10.1080/17455030.2021.1948627

Zhao, H., Li, C., Fu, Y., Oyarhossein, M.A., Habibi, M. and Safarpour, H. (2023), "Quasi-static indentation, low-velocity impact, and resonance responses of the laminated double-curved panel considering various boundary conditions", *Thin Wall. Struct.*, **183**, 110360. https://doi.org/10.1016/j.tws.2022.110360

Zhao, W., Suo, H., Wang, S., Ma, L., Wang, L., Wang, Q. and Zhang, Z. (2022), "Mg gas infiltration for the fabrication of MgB2 pellets using nanosized and microsized B powders", *J. Eur. Ceram. Soc.*, **42**(15), 7036-7048. https://doi.org/10.1016/j.jeurceramsoc.2022.08.029

Zhao, Y., Moradi, Z., Davoudi, M. and Zhuang, J. "Bending and stress responses of the hybrid axisymmetric system via state-space method and 3D-elasticity theory", *Eng. Comput.*, 1-23. https://doi.org/10.1007/s00366-020-01242-1

Zhao, Y., Moradi, Z., Davoudi, M. and Zhuang, J. (2021), "Bending and stress responses of the hybrid axisymmetric system via state-space method and 3D-elasticity theory", *Eng. Comput.*, 1-23. https://doi.org/10.1007/s00366-020-01242-1

Zheng, W., Liu, J., Oyarhossein, M.A., Safarpour, H. and Habibi, M. (2023), "Prediction of nth-order derivatives for vibration responses of a sandwich shell composed of a magneto-rheological core and composite face layers", *Eng. Anal. Bound. Elem.*, **146**, 170-183. https://doi.org/10.1016/j.enganabound.2022.10.019

Zheng, Y., Jin, H., Jiang, C., Moradi, Z., Khadimallah, M.A. and Moayedi, H. (2022), "Analyzing behavior of circular concrete-filled steel tube column using improved fuzzy models", *Steel Compos. Struct.*, **43**(5), 625-637. https://doi.org/10.12989/scs.2022.43.5.625

Zhou, C., Zhao, Y., Zhang, J., Fang, Y. and Habibi, M. (2020), "Vibrational characteristics of multi-phase nanocomposite reinforced circular/annular system", *Adv. Nano Res.*, **9**(4), 295-

307. https://doi.org/10.12989/anr.2020.9.4.295
Zhou, H., Xu, C., Lu, C., Jiang, X., Zhang, Z., Wang, J., Xiao, X., Xin, M. and Wang, L. (2021), "Investigation of transient magnetoelectric response of magnetostrictive/piezoelectric composite applicable for lightning current sensing", *Sensors Actuat A Phys*., **329**, 112789. https://doi.org/10.1016/j.sna.2021.112789
Zhou, J., Bai, J. and Liu, Y. (2022), "Fabrication and modeling of matching system for air-coupled transducer", *Micromachines*, **13**(5), 781. https://doi.org/10.3390/mi13050781.
Zhu, H. and Zhao, R. (2022), "Nucleation of CVD-prepared hexagonal boron nitride on Ni (100), Ni (110) and Ni (111) surfaces: A theoretical study", *Vacuum*, 111396. https://doi.org/10.1016/j.vacuum.2022.111396
Zhu, L., Ren, H., Habibi, M., Mohammed, K.J. and Khadimallah, M.A. (2022), "Predicting the environmental economic dispatch problem for reducing waste nonrenewable materials via an innovative constraint multi-objective Chimp Optimization Algorithm", *J. Clean. Prod*., 132697. https://doi.org/10.1016/j.jclepro.2022.132697